

# Construction and Validation of a Hybrid Lumbar Spine Model for the Fast Evaluation of Intradiscal Pressure and Mobility

Ali Hamadi Dicko, Nicolas Tong-Yette, Benjamin Gilles, François Faure, Olivier Palombi

**Abstract**—A novel hybrid model of the lumbar spine, allowing fast static and dynamic simulations of the disc pressure and the spine mobility, is introduced in this work. Our contribution is to combine rigid bodies, deformable finite elements, articular constraints, and springs into a unique model of the spine. Each vertebra is represented by a rigid body controlling a surface mesh to model contacts on the facet joints and the spinous process. The discs are modeled using a heterogeneous tetrahedral finite element model. The facet joints are represented as elastic joints with six degrees of freedom, while the ligaments are modeled using non-linear one-dimensional elastic elements. The challenge we tackle is to make these different models efficiently interact while respecting the principles of Anatomy and Mechanics.

The mobility, the intradiscal pressure, the facet joint force and the instantaneous center of rotation of the lumbar spine are validated against the experimental and theoretical results of the literature on flexion, extension, lateral bending as well as axial rotation.

Our hybrid model greatly simplifies the modeling task and dramatically accelerates the simulation of pressure within the discs, as well as the evaluation of the range of motion and the instantaneous centers of rotation, without penalizing precision. These results suggest that for some types of biomechanical simulations, simplified models allow far easier modeling and faster simulations compared to usual full-FEM approaches without any loss of accuracy.

**Keywords**—Hybrid, modeling, fast simulation, lumbar spine.

## I. INTRODUCTION

**T**HE human lumbar spine is an important and vital structure for which it is essential to propose models to accurately simulate it. It is a complex structure composed of nearly rigid parts : the vertebrae, and soft to stiff tissues : discs, facet joints, facet capsules, ligaments and muscles. Understanding the behavior of this system using computer simulations as well as *in vitro* and *in vivo* experiments is an important area of research in clinical applications, in treatment planning and in surgical training. Simulation aims at reproducing real phenomena in order to understand, to predict and to prevent serious health issues.

F. Faure and A. Dicko are with the Univ. Grenoble Alpes, INRIA Grenoble, France (e-mail : ali-hamadi.dicko@inria.fr)

O. Palombi and N. Tong-Yette are with the Univ. Grenoble Alpes, LADAF.  
B. Gilles are with the LIRMM-CNRS, INRIA.

It is therefore essential to propose models that accurately fit the anatomical and physiological description of each component and interactions that occur. However, traditional FEM simulations are notoriously hard to set up, due to geometrical complexity and the difficulty of trading off precision, which requires fine meshes, with computational efficiency, which requires simple models. Moreover, some applications such as medical and health-care hardware design, or numerical optimization are based on trial and error approaches involving numerous simulations, therefore computation time is also an important issue. To simulate the lumbar spine, two main approaches have been commonly taken.

On the one hand, full FEM approaches accurately compute local forces and deformations, which is especially useful for complex soft objects such as lumbar discs. Their agreement with experimental data from *in vitro* studies have been thoroughly tested [1–7]. However, they require volumetric meshes composed of well-shaped elements of all organs which can be difficult to build. Moreover, the resulting equation systems may be large, depending on the resolution of the meshes, resulting in slow computation times. These approaches commonly used are hard to set up, with numerous computational issues.

On the other hand, in motion studies, vertebra can be safely seen as rigid. These models composed of articulated rigid bodies are easier to set up and faster to simulate as demonstrated by several research work [8–10]. However they generally fail to accurately capture the relative motion between the vertebrae. Most of the spine studies involving simulation so far use either the FEM or the rigid body approaches. This may be due to the lack of software able to efficiently and accurately combine the two models, and to the lack of validation of such hybrid approaches.

To get the best of both worlds, we introduce a novel 3D dynamic model of the lumbar spine that combines both FEM and multibody systems.

While this intuitive idea is difficult to extensively trace back in the literature, the first general presentation of hybrid models was given by [11], using *hard bindings* or *soft bindings* to combine different models within the same object. This was later used to produce a detailed model of the upper body [12]. Alternatively, [13] showed that frame-based deformations with material-aware shape functions allow efficient hybrid models. This approach has been successfully applied to the simulation of the jaw-tongue-hyoid system [14]. Software is a major issue

for hybrid models.

The creation of a hybrid spine model is motivated by the need to address issues related to the accurate, efficient and fast simulation of intradiscal pressure, spine mobility, and motion quality through the evaluation of instantaneous center of rotation. While the evaluation of disc pressure requires accuracy, rigid body system is sufficient to compute spine mobility. Each vertebra is thus modeled using a rigid body with contact surface on zygapophyseal joints and on spinous process, while the facet joints are modeled using 6D elastic joints. The ligaments are modeled using non-linear springs attached to the vertebrae, and the discs are modeled using a heterogeneous finite element model. To emphasise our modeling choices, a specific attention is paid to the construction of the model. We validate the model by showing that our computations of the range of motion (ROM), the intradiscal pressure (IDP), the facet joint force (FJF) and the position of instantaneous center of rotation (ICR) are in agreement with the literature [15], *in vitro* and *in vivo* data. We show that accurate simulations of movements can be obtained with this easier modeling and faster computation times than using the traditional finite element method.

## II. MATERIAL AND METHOD

Our model of the lumbar spine is composed of the five lumbar vertebrae (L1-L5) that meet the sacral spine S1 on the base of L5 (see Fig. 1). Each pair of vertebrae are separated by an intervertebral disc and are connected by a pair of facet joints, and by a set of ligaments (see also Fig. 1). Geometry is taken from the bodyparts3d database [16]. We re-meshed these models to compute the FEM volumetric mesh of the discs (Fig. 2,3).

### A. Vertebrae

Vertebrae are usually divided in 6 segments : the vertebral body, the arch, the pedicles, the lamina, the transverse process and the spinous process, each of them attached to ligaments and muscles. Vertebrae transfer force of these elastic components within all the spine to enable its mobility and its stabilization. The main role of this bone is to bear and transfer compressive loads through its vertebral body. During most of the spine movements, contacts occur between the facet joints to limit these movements, and sometime, during the extension, a contact through the ligaments occurs between the spinous process of adjacent vertebrae to limit this specific movement.

Vertebrae are usually modeled using tetrahedron FE-model for the cancellous bone and hexahedra FE-model for the cortical bone [1],[4],[6],[7]. Since its deformations are negligible when studying motion, we model the vertebrae as rigid bodies connected to contact surfaces as illustrated in Fig. 2, since rigid bodies are enough to fulfill the functions of bearing load and transferring force. The surfaces of the spinous process and zygapophyseal joints create contacts between vertebrae during the movements of each functional spine units (FSU). Rigid bodies under go only three translations and three independent rotations, compared with three unknowns per mesh node in finite elements. This simplifies the equations,

and avoids numerical problems due to very high stiffness at the same time.

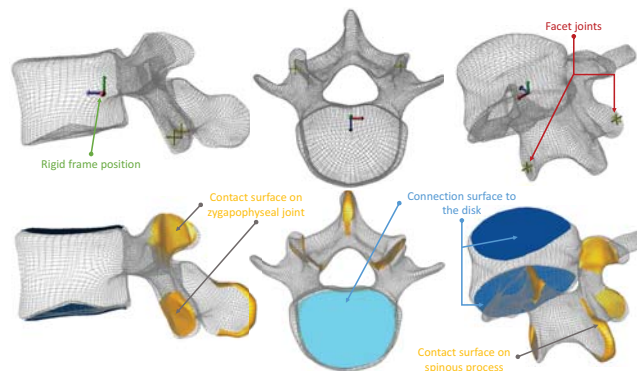


Fig. 2: Mechanical model of a vertebra. **Top** : the **rigid frame** that represent the vertebra, and in yellow on the top right **the two facet joint**. **Bottom** : The yellow surfaces are used to reproduce **the contact that occur between the adjacent vertebrae**. The blue surfaces are used to handle the connection between the vertebrae and the discs.

### B. Intervertebral Disc

Inter-vertebral discs are composed of four main parts : the annulus fibrosus, the nucleus pulposus and the two bony endplates that link it to the vertebrae (see Fig. 1). The inner portion, the nucleus pulposus, is a gelatinous mass located in the posterior part (Fig. 3). It is surrounded by the annulus fibrosus which is composed of fibrocartilage. The crisscross arrangement of the coarse collagen fiber bundles within the fibrocartilage allows the annulus fibrosus to withstand high bending and torsional loads. The endplates, composed hyaline cartilage, link the disc with the vertebrae. Discs are designed to bear and to distribute loads, and also to restrain excessive motion.

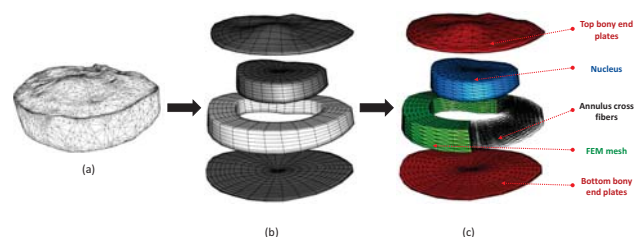


Fig. 3: Structure of inter-vertebral discs : the two endplates, the annulus and the nucleus. (a) : surface mesh from [16]. (b) : Subdivided and re-meshed version of disc surface. (c) : Our FEM mesh.

The inclusion of most of the anatomical and physiological aspects in disc model has been widely studied in previous work [3],[6],[7],[17],[18]. Our model keeps the subdivision of the disc in four components because of the large difference in the mechanical behavior and the role of each. For better computational efficiency, we modeled them using tetrahedral

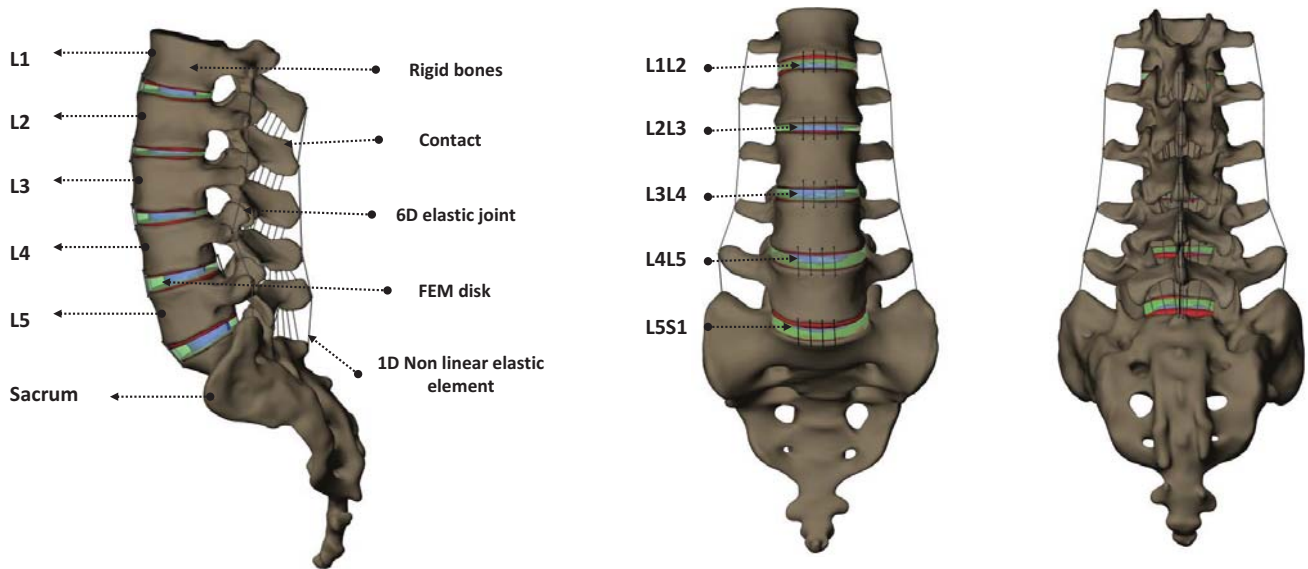


Fig. 1: Full model of the lumbar spine on the sacrum : vertebrae (L1-S1), intervetebral discs and ligaments. (a) Profile view. (b) Front view. (c) Bottom view.

Open Science Index, Medical and Health Sciences Vol:9, No:2, 2015 waset.org/Publication/10000566

solid elements (Fig. 3) with validated material parameters from the literature (cf Table. I). Because of the role of annulus fibers in the anisotropic deformations of this structure, and in the limitation of the lateral bending and the axial rotation movements [19], we add these fibers in the disc model to accurately capture deformations and pressures within this entity.

Since different models are used for vertebrae and discs, we have to pay special attention to anatomical constraints (namely perfect contact) and mechanical principles (namely two-way coupling). As noticed in [14], using Lagrange multipliers to attach FEM nodes to rigid objects would add computational complexity, while carefully leveraging these kinematic constraints actually allows to *simplify* the equations, by removing the attached nodes from the set of unknowns. We achieve this by introducing a diamond-shaped kinematic hierarchy, as illustrated in Fig. 4. The top node represents the whole object, with a dynamics solver. The two children contain the independent degrees of freedom (DOF) which include rigid frames for the vertebra, and only the free nodes of the FEM. The motions are propagated top-down through the hierarchy, while the forces are accumulated bottom-up. The FEM nodes attached to the vertebra are entirely controlled by the rigid motion of the vertebra. The multimapping takes input from the two particle sets and generates their union, at the bottom of the hierarchy. The FEM behavior laws such as inertia and stiffness are straightforwardly applied at the bottom level, making no difference between the particles. The inertia and elastic forces applied to these particles are mapped upward to their respective inputs. The particles mapped under the rigid body, in turn, accumulate their forces upward to the rigid bodies, where the rigid body inertia and forces (if any) are directly applied. This results in a two-way coupling with perfect attachment, while the elastic forces are automatically distributed to the independent DOFs.

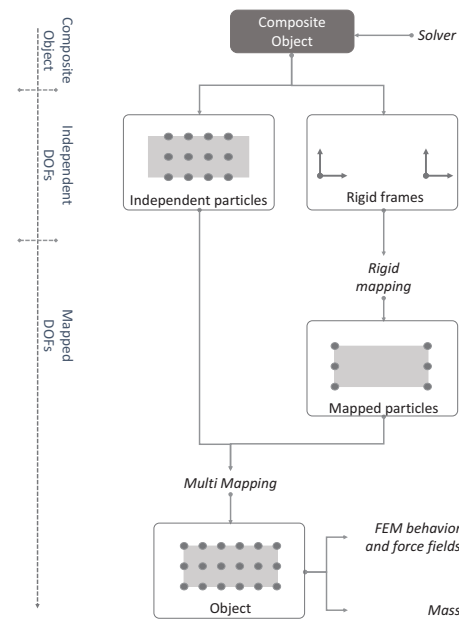


Fig. 4: Mechanical connection between the vertebrae and the discs.

### C. Zygapophyseal Joint

The zygapophyseal joints, also known as facet joints, are localized on the posterior part of the lumbar spine. They include the articular process of the two vertebrae that are coated with hyaline cartilage and surrounded by synovial fluid and the joint capsules. The capsules are composed of dense and parallel collagen fibers and irregularly oriented elastic fibers, which give them a mechanical behavior that reminds the behavior of ligaments hence the name capsular ligament. Their orientation determine the type of relative motion (flexion, extension, lateral bending but no axial rotation) between the vertebrae. It varies along the spine main segment [21], and

TABLE I  
 MECHANICAL PROPERTIES OF EACH COMPONENT OF THE MODEL

| Material            | Model choice                   | Parameter 1              | Parameter 2   | Element Type                 | Source |
|---------------------|--------------------------------|--------------------------|---|------------------------------|--------|
| <b>Vertebra</b>     |                                |                          |   |                              |        |
| Cancelous bone      | Rigid body                     |                          |   |                              |        |
| Cortical bone       |                                |                          |   |                              |        |
| <b>Disk</b>         |                                |                          |   |                              |        |
| Nucleus             | Linear Hooke                   | $E = 1MPa$               | $\nu = 0,49$  | Tetrahdra (4-node solid)     | [4]    |
| Annulus             | Hyperelastic Mooney Rivlin     | $c1=0.18,$<br>$c2=0.045$ |   | Tetrahdra (4-node solid)     | [1]    |
| Fibers of annulus   | Non-linear stress-strain curve |                          |   | 7 layers-criss-cross pattern | [19]   |
| EndPlate            | Linear Hooke                   | $E = 24MPa$              | $\nu = 0,4$   | Tetrahdra (4-node solid)     | [1]    |
| <b>Ligaments</b>    |                                |                          |   |                              |        |
| ALL                 | Non-linear stress-strain curve |                          |   | 1D spring (2-node link)      | [20]   |
| PLL                 | Non-linear stress-strain curve |                          |   | 1D spring (2-node link)      | [20]   |
| LF                  | Non-linear stress-strain curve |                          |   | 1D spring (2-node link)      | [20]   |
| TL                  | Non-linear stress-strain curve |                          |   | 1D spring (2-node link)      | [20]   |
| IL                  | Non-linear stress-strain curve |                          |   | 1D spring (2-node link)      | [20]   |
| SL                  | Non-linear stress-strain curve |                          |   | 1D spring (2-node link)      | [20]   |
| <b>Joints</b>       |                                |                          |   |                              |        |
| Facet joint capsule | Non-linear stress-strain curve |                          |   | 6D Elastic Element           | [4]    |
| Facet joint contact | Soft contact with friction     | $k=10, \text{coef}=0.1$  | alarm distance = 0.5mm,<br>contact distance = 0.1mm | Triangle surface mesh        |        |

from one person to another. The facet joints guide movement of each FSU and have load-bearing function [22].

Based on this, we choose elastic joints with six degree of freedom [23], three in translation and three in rotation, to model the elastic behavior of the capsules, with different stiffnesses for twist and stretch. To match to the anatomical position of the zygapophyseal joint, we set the elastic joints in the middle of the segment that pass through the centers of the two facets, as illustrated using yellow crosses in Fig. 2. Their material properties are set based on the literature [4].

#### D. Ligaments

The ligamentous apparatus of the spine mainly contributes to its intrinsic stability by allowing a balanced and restrained motion during the daily activities [5],[22]. Their composition provides the ligament with non-linear elasticity as shown in Fig. 5.

Our spine model includes six ligaments : the anterior longitudinal ligament (ALL), the posterior longitudinal ligament (PLL), the ligamentum flavum (FL), the transverse ligament (TL), the interspinous ligament (IL) and the supraspinous ligament (SL). Each ligament is modeled using a set of one-dimensional tension-only spring elements (black segments in Fig. 1), and its elastic behavior is defined by a strain-stress function. Differentiable stress-strain laws are necessary to efficient implicit numerical solvers [24], while the experimental laws described in the literature [4],[20] are composed of discrete sample points. We thus approximate these using sigmoid curves optimal in the least-square sense, which fit the data reasonably well as shown in Fig. 5.

### III. RESULTS AND VALIDATION

We base our validation protocol on those proposed in the work of Dreischarf et al [15] to show that our hybrid

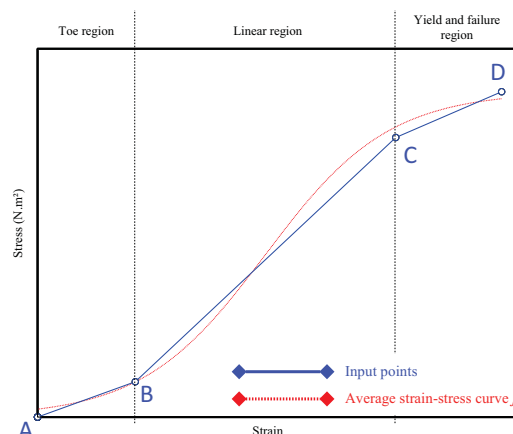


Fig. 5: Approximation of the stress-strain curve of a ligament. Blue: the input data defined by 4 points (A,B,C,D). Red: the corresponding approximated sigmoid function.

spine model reproduces the right ranges of motion (ROM), the right intradiscal pressures (IDP) and the right facet joint forces (FJF) according to the literature data, *in vitro* and *in vivo* measurements. This work of [15] presents eight validated and published models (*only the segment L1-L5*) of the literature, and compare the responses (i.e ROM, IDP and FJF) of these models when they are subject to pure and combined loading modes, the results are compared to *in vitro* and *in vivo* measurements. Thus, to perform the validation, we reproduce their experiments which are detailed below. To ease the readability, the models to whom we compare our spine model are renamed *model 1, model 2, ..., model 8*, and respectively correspond to those introduced in the following work : [3],[25–31]. To validate the location of the instantaneous center of rotation, we compare against those

obtained in [2],[32–34].

All the simulations were done using the SOFA library [35] on a laptop with a *Intel Bi-Core i7-3520M CPU @ 2.90GHz* and *8Go of RAM*. The dynamic simulations were performed with an implicit Euler integration scheme. To approximate the right solution, we use small time steps ( $dt=0.00001s$ ), and set the damping parameters of our implicit Euler solver to respectively 0.001 for the Rayleigh stiffness and 0 for the Rayleigh mass to avoid as much as possible the damping effects.

#### A. Validation under Pure Loading Mode :

For this first part of the validation, we use the segment L1-L5 since only this segment was used in the study of *Dreischarf et al* [15]. A fixation constraint is applied to the vertebra L5 to avoid all its possible displacements. Pure bending moment of  $7.5Nm$  is applied atop the vertebra L1 (cf Fig. 6), in the three anatomical planes (cf Fig. 7). The ROM and the FJF of our model are computed and compared to those obtained by [3],[25–31]. Facet joint forces are computed following a similar approach as [2].

Under pure moment, the hybrid spine model shows a ranges of motion that remain in the standard values of those found in the works to which the model is compared (cf Fig. 8.A). These ROM are also within the range of *in vivo* values (cf Fig. 8.A). In flexion-extension, it performs  $38^\circ$  where the median value of the literature FE-models is  $34^\circ$  with a range of value of  $24^\circ - 41^\circ$ . In axial rotation, our model shows  $18^\circ$  where the others FE-models performs an average angle of  $17^\circ(11^\circ - 22^\circ)$ . In lateral bending, our spine model perform a movement of  $41^\circ$  where the others FE-models performs a median angle of  $35^\circ(25^\circ - 41^\circ)$ .

The average facet joint forces of our model are 0 N in flexion,  $43N$  in extension (*median FE-models : 32N, range : 8N – 108N*), in lateral bending, it equals  $25N$  (*median FE-models : 12N, range : 5N – 41N*) and in axial rotation, it equals  $56N$  (*median FE-models : 87N, range : 37N – 134N*). As it is the case for the ROM, the FJF remain in the range of values founded in the literature as shown in Fig. 8.B.

Thereafter, the functional spine unit (FSU) L4-L5 is loaded under compression (from 0N to 1000N) and the IDP are compared to the IDP of the literature FE-models and the *in vitro* data. As in [15], we use the technique employed in [36] to avoid instability issues and to minimize artifact bending moments expected in compression loading. As emphasized for the models presented in [15], our model IDP increases almost linearly under the axial compressive forces as illustrated in Fig. 8.C. These IDP remain in the range of *in vitro* measurements.

#### B. Validation under Load Combinations:

For this part of the validation, as suggested in [15], the model is subject to compression in combination with bending and torsion. The loading modes are detailed in Table. II. The ROM, the IDP and the FJF are computed and compared to those obtained by [3],[25–31]. For each FSU, left and right FJF are average for the extension movement. In axial rotation

and lateral bending, for the evaluation the ROM, FJF and IDP, the side under higher load is chosen for the comparison [15].

TABLE II  
 LOADING MODES FOR THE SIMULATION OF DIFFERENT MOVEMENT

| Movement               | Compressive force (N) | Moment (Nm) |
|------------------------|-----------------------|-------------|
| <b>Flexion</b>         | 1175                  | 7,5         |
| <b>Extension</b>       | 500                   | 7,5         |
| <b>Lateral bending</b> | 700                   | 7,8         |
| <b>Axial rotation</b>  | 720                   | 5,5         |

Under load combination, the ROM of most of the FSU of our lumbar spine model are within the range of *in vivo* measurements as shown in Fig. 9, except for the flexion. In flexion, the resulting mobility is smaller than what is expected, taking into account *in vivo* data. However, this aspect is unfortunately present in all the model against which we compare our model (cf Fig. 9.A), and our ROM remain within the range of rotations performed by these FE-models. In lateral bending and in axial rotation, the movement amplitudes are close to those found in the literature and in the range of *in vivo* measurements as shown in Fig. 9.B, 9.C. In extension, such as for the other movements, ROM are within the range of movements performed by the other models and also within the range of *in vivo* measurements, except for the segment L4-L5 which performs a higher rotation than *in vivo* measure ( $4.2^\circ$  instead of the  $4^\circ$  expected) (cf Fig. 9.D).

The IDP of our model are within the range of IDP of the other models and close the median IDP of all these FE-models. In extension, lateral bending and axial rotation, the computed IDP are pretty close to *in vivo* IDP measured in the study of *Dreischarf et al* [15]. These IDP are all shown in detail in the Fig. 10.

Concerning the FJF, in flexion, they are null. This result confirms that the facet joints are unloaded as it is expected. During the extension, the lateral bending and the axial rotation, they are in the range of the FJF of the others FE-models, and they are mainly close to the median values of the FJF of these models (cf Fig. 11). Since no measurement with *in vitro* and *in vivo* data has been found, no comparison of these prediction against real data were possible.

#### C. Validation of ICR :

To validate the trajectory of the ICR, during each time step of the previous experiments, the centroids of each FSU during flexion, extension and the lateral bending are computed using the method proposed by [32] (Fig. 6.3). In our experiment, between 50 to 200 steps of simulation were performed. This large number of time step is motivated by the need of accurately following the motion of the centroid.

In flexion, each FSU predicts ICR position in a region that starts from the center of the intervertebral disc on its posterior part, then migrates posteriorly across the disc to finally ends its pathway in the upper region of the vertebral body of the bottom vertebra (cf right image in Fig. 12). The localization area of the ICR are consistent with the *in vivo* ICR computed by *Pearcy et al* [32] as shown in Fig. 12.A. Their trajectories

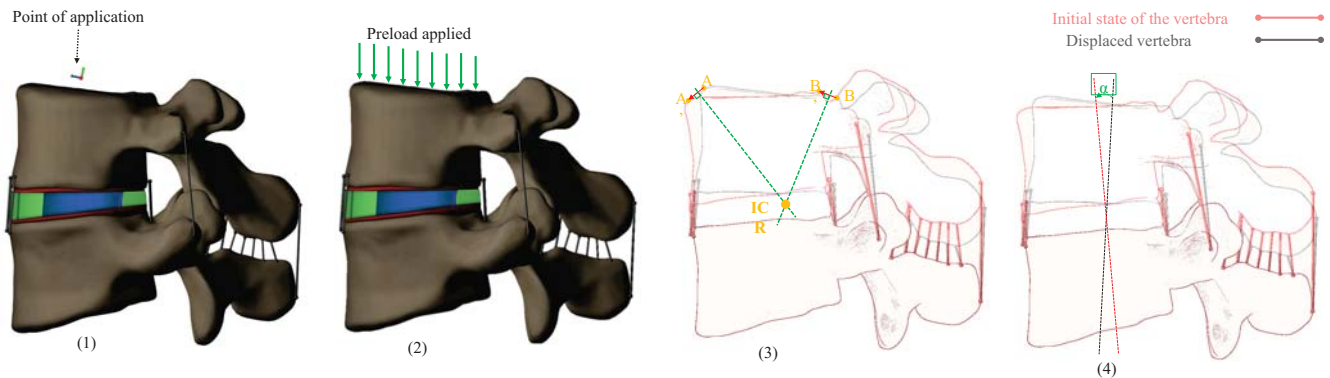


Fig. 6: Experimentation. (1) Point application of the pure moment. (2) Application of pre-load. (3) Computation of the ICR. (c) Computation of angle.

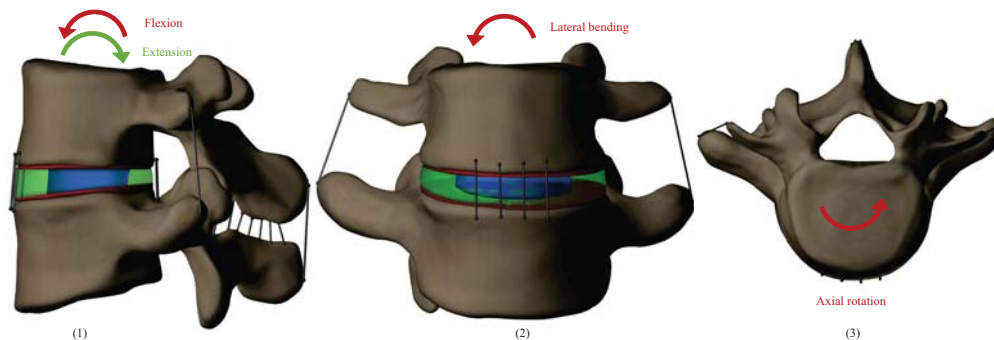


Fig. 7: Movements in the main anatomical plans. (1) Flexion - extension. (2) Lateral bending. (3) Axial rotation.

Open Science Index, Medical and Health Sciences Vol:9, No:2, 2015 waset.org/Publication/10000566

also fit the results obtained during a flexion by [33], [34] for L2-L3 and L5-S1, respectively.

During the extension, the FSU predicts ICR positions in a same area as the ICR of the flexion, but their trajectory during the extension are different (cf Fig. 12.B). The region of localization of these ICR is supported by the results obtained by [32]. For L2-L3, the centrodes obtained with the hybrid model have a same type of shape and are located in same area as those obtained by [34], the same observation can be applied for the segment L5-S1 if the comparison is made with the results obtained by [33].

In lateral bending, the ICR are located almost in the upper part of the disc, the shape of the trajectory reminds a bell shape that starts on the bottom part of the vertebral body, which continues across the disc until its center and then migrates toward the side of the bending (cf (D) in Fig. 12.D). The bell shape of the ICR and the area of the ICR position during a lateral bending are consistent with the results obtained by [2].

#### IV. DISCUSSION

The main objective of this work was to build a model of lumbar spine which enables a better computational efficiency while respecting anatomical and physiological description of this complex organ. The purposes are to evaluate intradiscal pressure, mobility and motion quality as fast as possible.

This interest in computational efficiency is motivated by the fact that numerous medical issues require some trial and error approaches (*e.g. inverse modeling, calibration process, etc*), involving numerous simulations. Not spending hours for each simulation thereby becomes increasingly beneficial. While rigid body systems are enough to evaluate the mobility, accurately compute intradiscal pressure require FE-models. Furthermore, evaluate the ICR mainly makes sense when disc is modeled and detailed, since they are used to evaluate motion quality and mainly if a disc is degenerated or intact [22]. Simulations usually works in two steps, the first one consisting in creating and validating a model, before starting the second step consisting in applying the model to address medical issues. This study represents the first step of this long process leading to the solving of bio-medical problems, and justifies why we focus first on validating our approach to simulate lumbar spine.

As [14], our results of simulations reported here demonstrate the effectiveness of the coupling between rigid bodies and finite element model. The model emphasize the assumption of simplifying the bones (vertebrae) as undeformable rigid bodies does not lead to a loss of accuracy in the quality of the movement, range of motion and intradiscal pressure produced by the lumbar segment in the three anatomical planes. The validations we provide show that model have a physiological

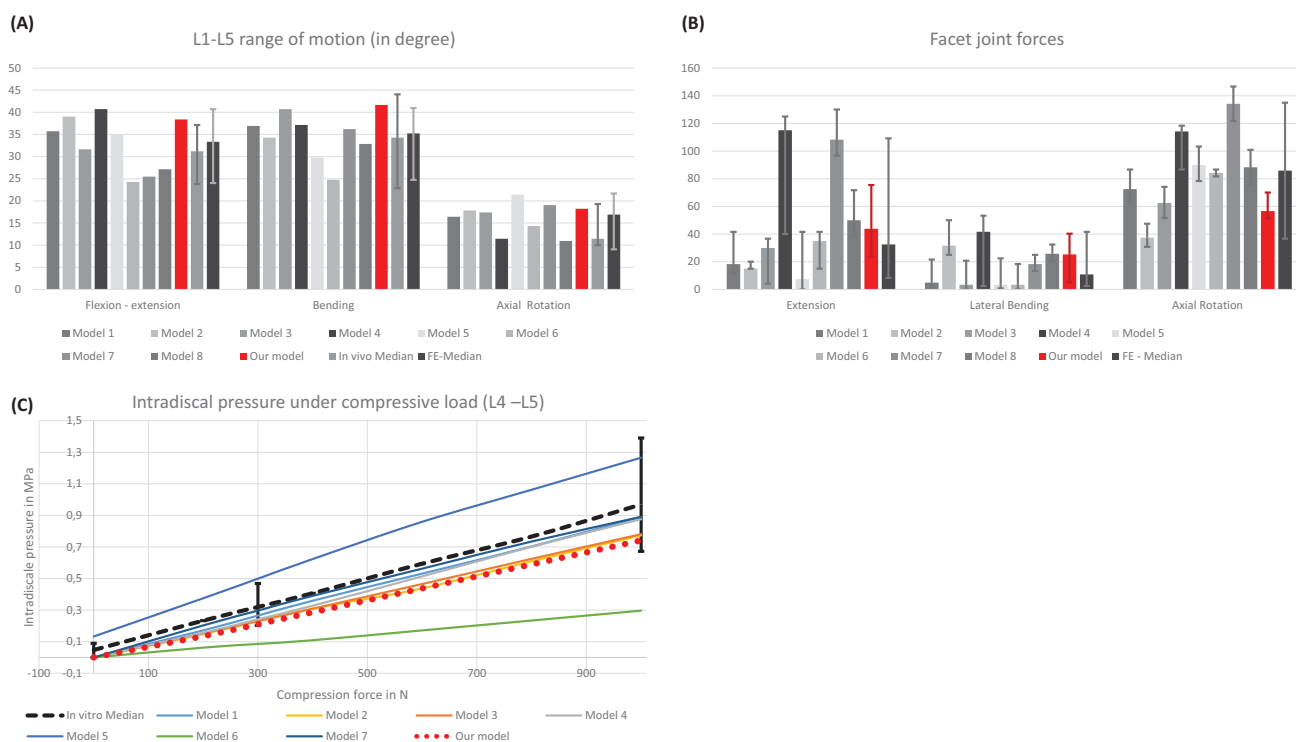


Fig. 8: (A) Range of motion under pure moments, our model is represent by the red bar. (B) Median facet joint forces of the segment L1-L5 under pure moments, our model is represent by the red bar. (C) Variation of intradiscal pressure in L4-L5 according to variation force. Our model is represented by the red dotted line.

movement with amplitudes of movement which remain within the range of what is performed by the models of the literature. We also show that the model is in agreement *in vitro* and *in vivo* measurements. More than validating only the kinematic of the model, we also show that the model reproduces IDP and FJF which are in agreement with predication of other FE-models and measurements from real human.

Despite the difference in the load and the force transfer we can observe between an FEM and a rigid body more generally, our hybrid segment of spine shows through the ICR trajectories the quality of the movement of the model which is a consequence of the transfer function within the spine segments. These results are supported by the *in vitro* and simulation experimentations of further works. It is interesting to notice that these nice movements are largely due to the behaviour of the zygapophyseal joint that confirmed that these entities can be represented as elastic joints with six degree of freedom per joint : three translations and three rotations.

The main advantages of the hybrid model is first of all its construction, the only entities that require a meshing stage are the disks, and it is well known that this step is usually time consuming and a complex task. Create different configurations for medical experiment become easier and quicker than using traditionnal FE-approaches. The position of the rigid body, and all the parameters that describes each vertebra are automatically computed based on the geometrical shape of each bone. An other advantage of the model is the computation time of the simulation. The simulation of one

FSU from the beginning of the movement until its stabilisation spend less than 7 seconds, and the simulation runs in real time. For the simulation of the whole spine, the simulation took less than 6 minutes from the beginning until the stabilisation. The acceleration of the computation time is mostly due to the lower number of degree of freedom that the model contains. Since we did not find any computation time in the literature works, we rely on the number of nodes per model to estimate the gain in time. The FSU L4-L5 made by [5] contains 270 324 solid elements for the disc and the two vertebrae, while for the same FSU our model only required 5038 solid elements for an equivalent results. Concerning computation time, using our simulator, the simulation of 5038 nodes runs at 8 frames per seconde (FPS), where the simulation of 30000 nodes runs at 0.7FPS, a model with 270000 nodes will run even slower.

However, our hybrid model presents some limitations. It is not the most suitable representation of the spine for some studies like the impact of the bone porosity in the spine transfer function or any study that involves some changes in the internal behaviour of the vertebra. Except such cases, our hybrid lumbar spine best suited numerous other studies with its easier and quicker modeling process due to the lower number of input parameter and DOF.

## V. CONCLUSION

We have presented a novel hybrid model of the lumbar spine which combines both rigid bodies and FEM in the same model for the sake of computational efficiency. We described

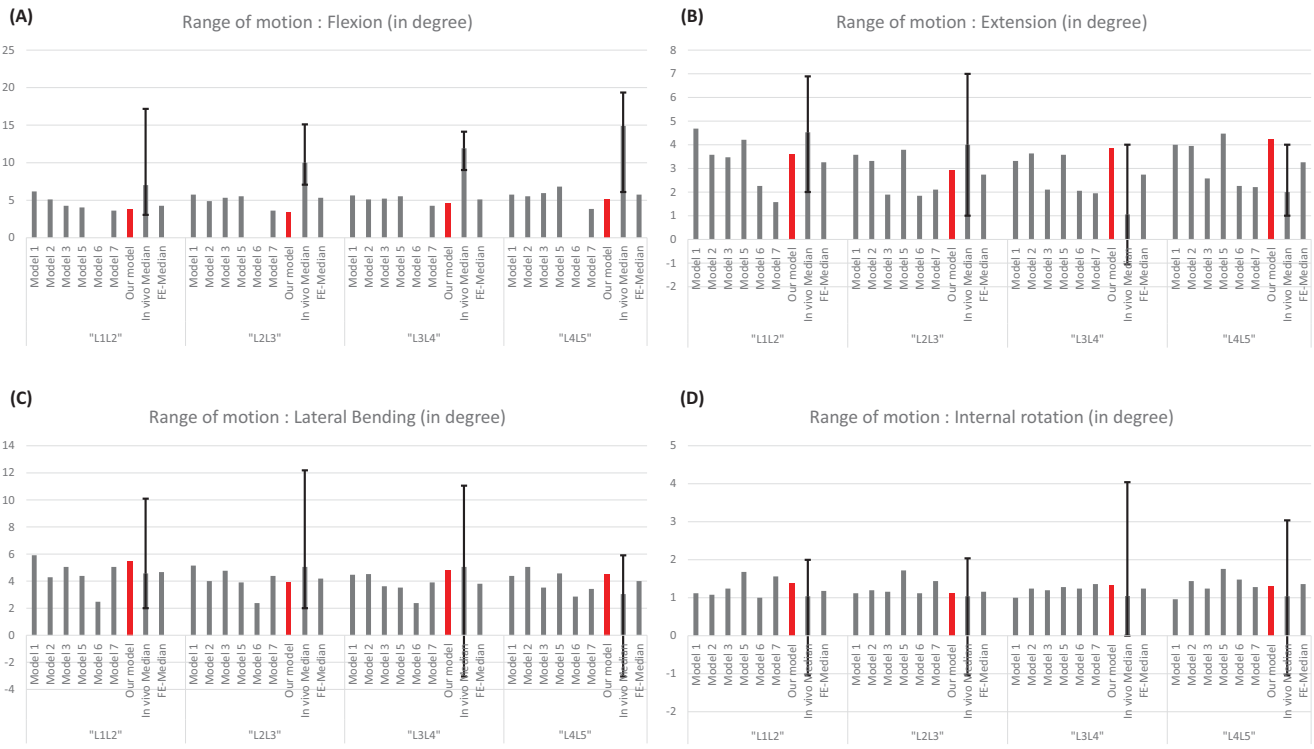


Fig. 9: Comparison of range of motion, our model is represented by the red bar. (A) Flexion. (B) Extension. (C) Lateral bending. (D) Axial rotation. Angles are in degree.

how the model have been constructed based on the anatomical and physiological behaviour of this segment of spine. The model has been validated in agreement with the literature. This stage of construction and validation of the model was the first step before its use for medical and biomechanical purposes. In future work, we plan to experiment mesh-less, frame-based deformations [13], to remove the last stage of meshing that remains in our modeling process and further accelerate the computations.

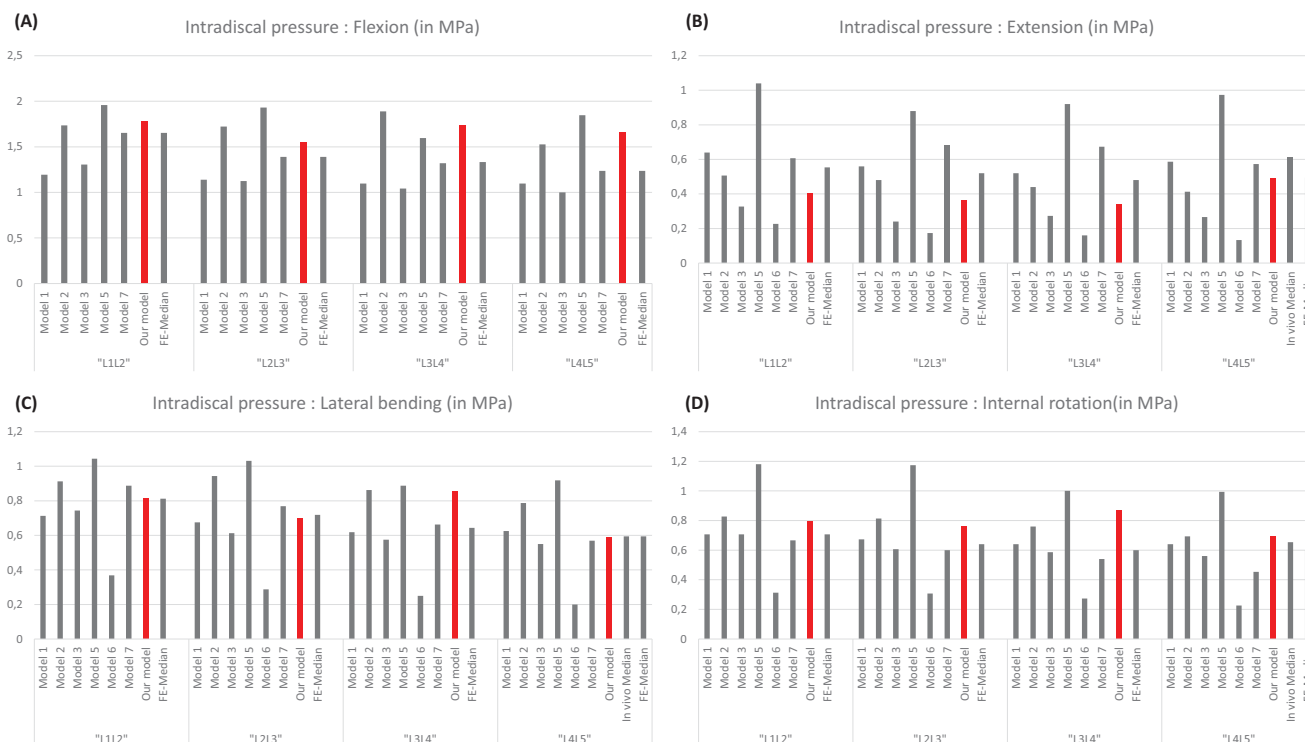


Fig. 10: Comparison of intradiscal pressure, our model is represented by the red bar. (A) Flexion. (B) Extension. (C) Lateral bending. (D) Axial rotation.

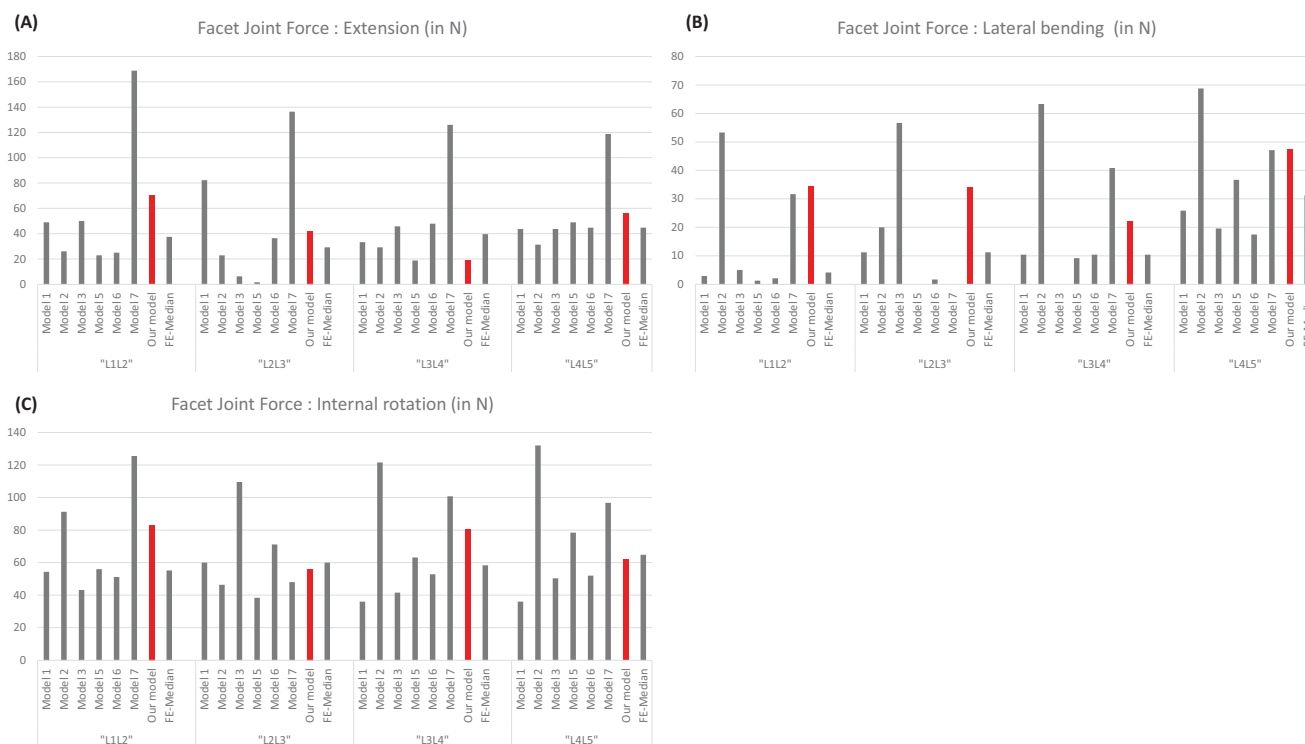


Fig. 11: Comparison of facet joint forces, our model is represented by the red bar. (A) Flexion. (B) Extension. (C) Lateral bending. (D) Axial rotation

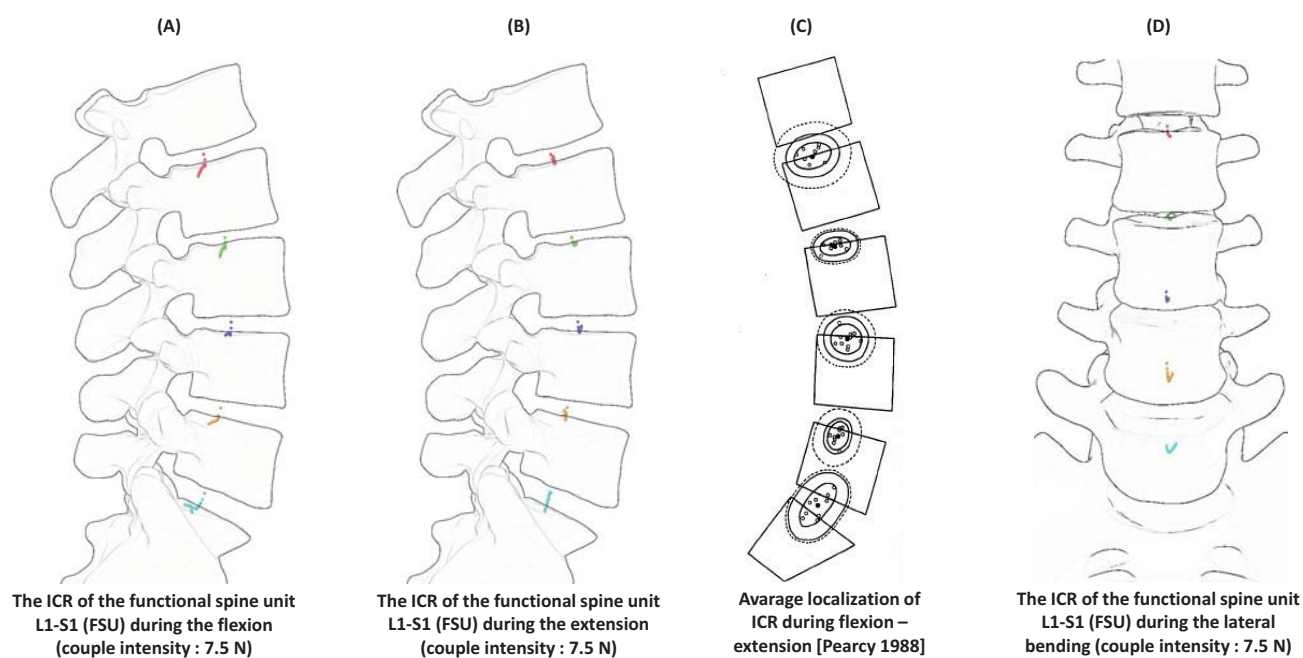


Fig. 12: Comparison of instantaneous center of rotation location. **A** : hybrid model ICR in during the flexion. **B** : hybrid model ICR in during the extension. **C** : ICR location computed in [32]. **D** : hybrid model ICR in during the lateral bending.

#### ACKNOWLEDGMENT

Many thanks to Laura Paiardini and Estelle Charleroy. This research work has been grant by the ANR SoHuSim.

#### REFERENCES

- [1] H. Schmidt, F. Heuer, J. Drumm, Z. Klezl, L. Claes, and H.-J. Wilke, "Application of a calibration method provides more realistic results for a finite element model of a lumbar spinal segment." *Clinical biomechanics (Bristol, Avon)*, vol. 22, no. 4, pp. 377–84, May 2007. [Online]. Available: <http://www.ncbi.nlm.nih.gov/pubmed/17204355>
- [2] H. Schmidt, F. Heuer, L. Claes, and H.-J. Wilke, "The relation between the instantaneous center of rotation and facet joint forces - A finite element analysis." *Clinical biomechanics (Bristol, Avon)*, vol. 23, no. 3, pp. 270–8, Mar. 2008. [Online]. Available: <http://www.ncbi.nlm.nih.gov/pubmed/17997207>
- [3] H. Schmidt, F. Galbusera, A. Rohlmann, T. Zander, and H.-J. Wilke, "Effect of multilevel lumbar disc arthroplasty on spine kinematics and facet joint loads in flexion and extension: a finite element analysis." *European Spine Journal*, vol. 21, no. 5, pp. 663–674, 2012. [Online]. Available: <http://dx.doi.org/10.1007/s00586-010-1382-1>
- [4] D. S. Shin, K. Lee, and D. Kim, "Biomechanical study of lumbar spine with dynamic stabilization device using finite element method," *Comput. Aided Des.*, vol. 39, no. 7, pp. 559–567, Jul. 2007. [Online]. Available: <http://dx.doi.org/10.1016/j.cad.2007.03.005>
- [5] Y. Alapan, C. Demir, T. Kaner, R. Guclu, and S. Inceoglu, "Instantaneous center of rotation behavior of the lumbar spine with ligament failure." *Journal of neurosurgery. Spine*, vol. 18, no. 6, pp. 617–26, Jun. 2013. [Online]. Available: <http://www.ncbi.nlm.nih.gov/pubmed/23600587>
- [6] T. Zander, A. Rohlmann, and G. Bergmann, "Influence of ligament stiffness on the mechanical behavior of a functional spinal unit." *Journal of biomechanics*, vol. 37, no. 7, pp. 1107–11, Jul. 2004. [Online]. Available: <http://www.ncbi.nlm.nih.gov/pubmed/15165881>
- [7] B. Weisse, a. K. Aiyangar, C. Affolter, R. Gander, G. P. Terrasi, and H. Ploeg, "Determination of the translational and rotational stiffnesses of an L4-L5 functional spinal unit using a specimen-specific finite element model." *Journal of the mechanical behavior of biomedical materials*, vol. 13, pp. 45–61, Sep. 2012. [Online]. Available: <http://www.ncbi.nlm.nih.gov/pubmed/22842275>
- [8] T. Yoshimura, K. Nakai, and G. Tamaoki, "Multi-body dynamics modelling of seated human body under exposure to whole-body vibration." *Industrial health*, vol. 43, no. 3, pp. 441–7, Jul. 2005. [Online]. Available: <http://www.ncbi.nlm.nih.gov/pubmed/16100921>
- [9] M. Christophy, N. Faruk Senan, J. Lotz, and O. O'Reilly, "A musculoskeletal model for the lumbar spine," *Biomechanics and Modeling in Mechanobiology*, vol. 11, no. 1-2, pp. 19–34, 2012. [Online]. Available: <http://dx.doi.org/10.1007/s10237-011-0290-6>
- [10] K. T. Huynh, I. Gibson, B. N. Jagdish, and W. F. Lu, "Development and validation of a discretised multi-body spine model in LifeMOD for biodynamic behaviour simulation." *Computer methods in biomechanics and biomedical engineering*, vol. 0, no. June 2013, pp. 37–41, Apr. 2013. [Online]. Available: <http://www.ncbi.nlm.nih.gov/pubmed/23621475>
- [11] E. Sifakis, T. Shinar, G. Irving, and R. Fedkiw, "Hybrid simulation of deformable solids," in *Proceedings of the 2007 ACM SIGGRAPH/Eurographics symposium on Computer animation*. Eurographics Association, 2007, pp. 81–90.
- [12] S.-H. Lee, E. Sifakis, and D. Terzopoulos, "Comprehensive biomechanical modeling and simulation of the upper body," *ACM Trans. Graph.*, vol. 28, no. 4, pp. 99:1–99:17, Sep. 2009. [Online]. Available: <http://doi.acm.org/10.1145/1559755.1559756>
- [13] F. Faure, B. Gilles, G. Bousquet, and D. K. Pai, "Sparse meshless models of complex deformable solids," *ACM Trans. Graph.*, vol. 30, no. 4, pp. 73:1–73:10, Jul. 2011. [Online]. Available: <http://doi.acm.org/10.1145/2010324.1964968>
- [14] I. Stavness, J. E. Lloyd, Y. Payan, and S. Fels, "Coupled hard-soft tissue simulation with contact and constraints applied to jaw-tongue-hyoid dynamics," *International Journal for Numerical Methods in Biomedical Engineering*, vol. 27, no. 3, pp. 367–390, 2011.
- [15] M. Dreischarf, T. Zander, A. Shirazi-Adl, C. Puttlitz, C. Adam, C. Chen, V. Goel, A. Kiapour, Y. Kim, K. Labus *et al.*, "Comparison of eight published static finite element models of the intact lumbar spine: Predictive power of models improves when combined together," *Journal of biomechanics*, vol. 47, no. 8, pp. 1757–1766, 2014.
- [16] N. Mitsuhashi, K. Fujieda, T. Tamura, S. Kawamoto, T. Takagi, and K. Okubo, "Bodyparts3d: 3d structure database for anatomical concepts," *Nucleic Acids Research*, vol. 37, no. suppl 1, pp. D782–D785, 2009.
- [17] S. J. Ferguson, K. Ito, and L.-P. Nolte, "Fluid flow and convective transport of solutes within the intervertebral disc," *Journal of Biomechanics*, vol. 37, no. 2, pp. 213 – 221, 2004, spinal Biomechanics. [Online]. Available: <http://www.sciencedirect.com/science/article/pii/S0021929003002501>
- [18] A. Malandrino, J. A. Planell, and D. Lacroix, "Statistical factorial analysis on the poroelastic material properties sensitivity of the lumbar intervertebral disc under compression, flexion and axial rotation," *Journal of Biomechanics*, vol. 42, no. 16, pp. 2780 – 2788, 2009. [Online]. Available: <http://www.sciencedirect.com/science/article/pii/S0021929009004679>
- [19] A. Shirazi-Adl, A. M. AHMED, and S. C. SHRIVASTAVA, "Mechanical response of a lumbar motion segment in axial torque alone and combined with compression," *Spine*, vol. 11, no. 9, pp. 914–927,

- 1986.
- [20] J. Chazal, a. Tanguy, M. Bourges, G. Gaurel, G. Escande, M. Guillot, and G. Vanneville, "Biomechanical properties of spinal ligaments and a histological study of the supraspinal ligament in traction." *Journal of biomechanics*, vol. 18, no. 3, pp. 167–76, Jan. 1985. [Online]. Available: <http://www.ncbi.nlm.nih.gov/pubmed/3997901>
- [21] Y. Masharawi, B. Rothschild, G. Dar, S. Peleg, D. Robinson, E. Been, and I. Hershkovitz, "Facet Orientation in the Thoracolumbar Spine: Three-dimensional Anatomic and Biomechanical Analysis," *Spine*, vol. 29, no. 16, 2004. [Online]. Available: [http://journals.lww.com/spinejournal/Fulltext/2004/08150/Facet\\\_Orientation\\\_in\\\_the\\\_Thoracolumbar\\\_Spine\\\_9.aspx](http://journals.lww.com/spinejournal/Fulltext/2004/08150/Facet\_Orientation\_in\_the\_Thoracolumbar\_Spine\_9.aspx)
- [22] M. Nordin and V. H. V. H. Frankel, *Basic biomechanics of the musculoskeletal system*. Philadelphia (Pa.): Lippincott Williams & Wilkins, 2001. [Online]. Available: <http://opac.inria.fr/record=b1133407>
- [23] A. De Luca, "Feedforward/feedback laws for the control of flexible robots," in *Robotics and Automation, 2000. Proceedings. ICRA '00. IEEE International Conference on*, vol. 1, 2000, pp. 233–240 vol.1.
- [24] W. H. Press, S. A. Teukolsky, W. T. Vetterling, and B. P. Flannery, *Numerical Recipes 3rd Edition: The Art of Scientific Computing*, 3rd ed. New York, NY, USA: Cambridge University Press, 2007.
- [25] W. M. Park, K. Kim, and Y. H. Kim, "Effects of degenerated intervertebral discs on intersegmental rotations, intradiscal pressures, and facet joint forces of the whole lumbar spine," *Computers in biology and medicine*, vol. 43, no. 9, pp. 1234–1240, 2013.
- [26] U. M. Ayturk and C. M. Puttlitz, "Parametric convergence sensitivity and validation of a finite element model of the human lumbar spine," *Computer methods in biomechanics and biomedical engineering*, vol. 14, no. 8, pp. 695–705, 2011.
- [27] C.-L. Liu, Z.-C. Zhong, H.-W. Hsu, S.-L. Shih, S.-T. Wang, C. Hung, and C.-S. Chen, "Effect of the cord pretension of the dynesys dynamic stabilisation system on the biomechanics of the lumbar spine: a finite element analysis," *European Spine Journal*, vol. 20, no. 11, pp. 1850–1858, 2011.
- [28] J. P. Little, H. De Visser, M. J. Pearcy, and C. J. Adam, "Are coupled rotations in the lumbar spine largely due to the osseo-ligamentous anatomy?—a modeling study," *Computer methods in biomechanics and biomedical engineering*, vol. 11, no. 1, pp. 95–103, 2008.
- [29] A. Shirazi-Adl, "Biomechanics of the lumbar spine in sagittal/lateral moments," *Spine*, vol. 19, no. 21, pp. 2407–2414, 1994.
- [30] T. Zander, A. Rohlmann, and G. Bergmann, "Influence of different artificial disc kinematics on spine biomechanics," *Clinical biomechanics*, vol. 24, no. 2, pp. 135–142, 2009.
- [31] A. Kiapour, D. Ambati, R. W. Hoy, and V. K. Goel, "Effect of graded facetectomy on biomechanics of dynesys dynamic stabilization system," *Spine*, vol. 37, no. 10, pp. E581–E589, 2012.
- [32] M. J. PEARCY and N. BOGDUK, "Instantaneous Axes of Rotation of the Lumbar Intervertebral Joints," *Spine*, vol. 13, no. 9, 1988. [Online]. Available: [http://journals.lww.com/spinejournal/Fulltext/1988/09000/Instantaneous\\\_Axes\\\_of\\\_Rotation\\\_of\\\_the\\\_Lumbar.11.aspx](http://journals.lww.com/spinejournal/Fulltext/1988/09000/Instantaneous\_Axes\_of\_Rotation\_of\_the\_Lumbar.11.aspx)
- [33] M.-A. Rousseau, D. S. Bradford, T. M. Hadi, K. L. Pedersen, and J. C. Lotz, "The instant axis of rotation influences facet forces at L5/S1 during flexion/extension and lateral bending," *European spine journal : official publication of the European Spine Society, the European Spinal Deformity Society, and the European Section of the Cervical Spine Research Society*, vol. 15, no. 3, pp. 299–307, Mar. 2006. [Online]. Available: <http://www.pubmedcentral.nih.gov/articlerender.fcgi?artid=3489304&tool=pmcentrez&rendertype=abstract>
- [34] P. Bifulco, M. Cesarelli, T. Cerciello, and M. Romano, "A continuous description of intervertebral motion by means of spline interpolation of kinematic data extracted by videofluoroscopy." *Journal of biomechanics*, vol. 45, no. 4, pp. 634–41, Feb. 2012. [Online]. Available: <http://www.ncbi.nlm.nih.gov/pubmed/22277152>
- [35] Faure, F., Duriez, C., Delingette, H., Allard, J., Gilles, B., Marchesseau, S., Talbot, H., Courtecuisse, H., Bousquet, G., Peterlik, I. and Cotin S., "SOFA: A Multi-Model Framework for Interactive Physical Simulation," *Soft Tissue Biomechanical Modeling for Computer Assisted Surgery*, vol. 11, pp. 283–321, 2012.
- [36] A. Shirazi-Adl and M. Parnianpour, "Load-bearing and stress analysis of the human spine under a novel wrapping compression loading," *Clinical Biomechanics*, vol. 15, no. 10, pp. 718–725, 2000.